

# Understanding the kinetics of the ClO dimer cycle

M. von Hobe<sup>1</sup>, R. J. Salawitch<sup>2</sup>, T. Canty<sup>2</sup>, H. Keller-Rudek<sup>3</sup>, G. K. Moortgat<sup>3</sup>,  
 J.-U. Grooß<sup>1</sup>, R. Müller<sup>1</sup>, and F. Stroh<sup>1</sup>

<sup>1</sup>Forschungszentrum Jülich GmbH, Institute for Chemistry and Dynamics of the Geosphere (ICG-I), Jülich, Germany

<sup>2</sup>Jet Propulsion Laboratory, California Institute of Technology, Pasadena, California, USA

<sup>3</sup>Max-Planck-Institute for Chemistry, Atmospheric Chemistry Division, Mainz, Germany

Received: 12 June 2006 – Accepted: 7 July 2006 – Published: 14 August 2006

Correspondence to: M. von Hobe (m.von.hobe@fz-juelich.de)

7905

## Abstract

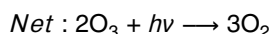
Among the major factors controlling ozone loss in the polar winter is the kinetics of the ClO dimer catalytic cycle. The most important issues are the thermal equilibrium between ClO and Cl<sub>2</sub>O<sub>2</sub>, the rate of Cl<sub>2</sub>O<sub>2</sub> formation, and the Cl<sub>2</sub>O<sub>2</sub> photolysis rate. All these issues have been addressed in a large number of laboratory, field and theoretical studies, but large discrepancies between individual results exist and a self-consistent set of parameters compatible with field observations of ClO and Cl<sub>2</sub>O<sub>2</sub> has not been identified. Here, we use thermodynamic calculations and unimolecular rate theory to constrain the ClO/Cl<sub>2</sub>O<sub>2</sub> equilibrium constant and the rate constants for Cl<sub>2</sub>O<sub>2</sub> formation and dissociation. This information is used together with available atmospheric data to examine Cl<sub>2</sub>O<sub>2</sub> photolysis rates based on different Cl<sub>2</sub>O<sub>2</sub> absorption cross sections. Good overall consistency is achieved using a ClO/Cl<sub>2</sub>O<sub>2</sub> equilibrium constant recently suggested by Plenge et al. (2005), the Cl<sub>2</sub>O<sub>2</sub> recombination rate constant reported by Nikolaisen et al. (1994) and Cl<sub>2</sub>O<sub>2</sub> photolysis rates based on averaged absorption cross sections that are roughly intermediate between the JPL 2002 assessment and a laboratory study by Burkholder et al. (1990).

## 1 Introduction

The ClO dimer cycle is one of the most important catalytic cycles destroying ozone in the polar vortices in late winter/early spring (Molina and Molina, 1987):



7906



In darkness thermal equilibrium of Reaction+ (R1) is established with

$$K_{\text{eq}} = \frac{k_{\text{rec}}}{k_{\text{diss}}} = \frac{[\text{Cl}_2\text{O}_2]}{[\text{ClO}]^2} \quad (1)$$

5 The terms  $k_{\text{rec}}$  and  $k_{\text{diss}}$  refer to rate constants for the recombination of ClO and ClO and the dissociation of ClOOCl, respectively;  $K_{\text{eq}}$  refers to the equilibrium constant. When light is available  $\text{Cl}_2\text{O}_2$  (unless stated otherwise,  $\text{Cl}_2\text{O}_2$  here refers to the chlorine peroxide isomer, ClOOCl, the only isomer that leads to ozone loss upon photolysis) is readily photolysed, and it has been demonstrated that between 90 and 100% of the  
10 product yield is comprised of Cl and ClOO as in Reaction (R2), out to wavelengths of 308 nm (Moore et al., 1999; Plenge et al., 2004). No laboratory measurements of product yields are available for wavelengths longer than 308 nm, which represents a considerable gap in laboratory confirmation of ozone loss by the ClO+ClO cycle. For a given amount of active chlorine ( $[\text{ClO}_x] \sim [\text{ClO}] + 2[\text{Cl}_2\text{O}_2]$ ) the rate at which this  
15 catalytic cycle destroys ozone is determined by the dimer formation rate constant  $k_{\text{rec}}$  and the photolysis rate  $J$ , which depends directly on the actinic flux and the absorption cross section  $\sigma_{\text{ClOOCl}}$ . The combined ozone loss rate from all catalytic cycles (see e.g. Solomon, 1999) is more sensitive to  $J$  than to  $k_{\text{rec}}$ : increasing  $J$  leads to a faster dimer cycle as well as to higher [ClO], which largely determines the rates of other  
20 catalytic cycles, in particular the ClO-BrO cycle (McElroy et al., 1986). On the other hand, the enhanced overall rate of the dimer cycle induced by increasing  $k_{\text{rec}}$  is partly offset due to the effect of reduced [ClO] on other catalytic cycles.

A large number of laboratory studies have addressed  $K_{\text{eq}}$  (Basco and Hunt, 1979; Cox and Hayman, 1988; Nickolaisen et al., 1994; Ellermann et al., 1995; Plenge et al.,  
25 2005),  $k_{\text{rec}}$  (Sander et al., 1989; Troler et al., 1990; Nickolaisen et al., 1994; Bloss et al., 2001; Boakes et al., 2005) and  $\sigma_{\text{ClOOCl}}$  (Basco and Hunt, 1979; Molina and Molina, 1997; 7907

1987; Permien et al., 1988; Cox and Hayman, 1988; DeMore and Tschuikow-Roux, 1990; Burkholder et al., 1990; Huder and DeMore, 1995). For each of these parameters, large discrepancies exist, and some proposed values for individual parameters or combinations thereof are inconsistent in the thermodynamic properties they imply  
5 (Golden, 2003). The consistency with atmospheric observations has been tested extensively (Shindell and de Zafra, 1995; Shindell and de Zafra, 1996; Solomon et al., 2000; Avallone and Toohey, 2001; Solomon et al., 2002; Stimpfle et al., 2004; von Hobe et al., 2005) showing that some of the constants determined in the laboratory cannot be reconciled with atmospheric [ClO] and  $[\text{Cl}_2\text{O}_2]$ . Taken together, this results  
10 in rather large uncertainties being reported for these constants by Sander et al. (2003) in the JPL recommendations, referred to as JPL 2002 in the following.

The aim of this study is to reduce these uncertainties and identify a set of values for  $K_{\text{eq}}$ ,  $k_{\text{rec}}$  and  $\sigma_{\text{ClOOCl}}$  that are consistent with each other and with atmospheric observations while still being reconcilable with theoretically feasible thermodynamic and  
15 energy transfer properties. We start by using statistical thermodynamics to constrain  $K_{\text{eq}}$ , and exploit the result together with corresponding thermodynamic properties to successively constrain  $k_{\text{diss}}$  and  $k_{\text{rec}}$  with the help of unimolecular rate theory as developed by Troe (1977a, b; 1979). With these parameters fixed,  $\text{Cl}_2\text{O}_2$  photolysis rates are estimated from simultaneous ClO and  $\text{Cl}_2\text{O}_2$  observations assuming photochemical steady state. To test this assumption, calculations with a chemical box model are  
20 also carried out.

## 2 Enthalpies and entropies of ClO and $\text{Cl}_2\text{O}_2$ and the equilibrium constant $K_{\text{eq}}$

The equilibrium of Reaction (R1) and its temperature dependence have been addressed in numerous studies. Laboratory measurements of  $K_{\text{eq}}$  have been carried  
25 out by Basco and Hunt, (1979), Cox and Hayman (1988), Nickolaisen et al. (1994) and Ellermann et al. (1995). Avallone and Toohey (2001) and von Hobe et al. (2005) have inferred  $K_{\text{eq}}$  from field observations of ClO and  $\text{Cl}_2\text{O}_2$ . A value for  $K_{\text{eq}}$  was de-

terminated from analysis of atmospheric measurements of ClO and Cl<sub>2</sub>O<sub>2</sub> by von Hobe et al. (2005). Avallone and Toohey (2001) also estimated a value for  $K_{eq}$ , based on atmospheric measurements of ClO and estimates of the concentration of Cl<sub>2</sub>O<sub>2</sub> found using an assumption of complete chlorine activation.

5  $K_{eq}$  is related to the standard reaction enthalpy  $\Delta_r H^\circ$  and entropy  $\Delta_r S^\circ$ :

$$K_{eq} = \frac{RT}{N_A} e^{\Delta_r S^\circ / R} e^{-\Delta_r H^\circ / RT} \quad (2)$$

with the factor  $RT/N_A$  ( $R$  in cm<sup>3</sup> atm K<sup>-1</sup> mol<sup>-1</sup>) converting  $K_{eq}$  into units of molecules<sup>-1</sup> cm<sup>3</sup>.  $\Delta_r S^\circ$  can be calculated from the third law entropies of ClO and Cl<sub>2</sub>O<sub>2</sub> (see below).  $\Delta_r H^\circ$  has been determined in the laboratory (Plenge et al., 2005) and estimated in ab initio calculations (McGrath et al., 1990; Lee et al., 1992; Zhu and Lin, 2003).

10 The kinetic laboratory studies (Cox and Hayman, 1988; Nickolaissen et al., 1994) can be interpreted either by third law analysis (i.e. obtaining  $\Delta_r S^\circ$  from third law entropies and fitting  $\Delta_r H^\circ$ ) or by second law analysis (i.e. both  $\Delta_r H^\circ$  and  $\Delta_r S^\circ$  are obtained from a linear least squares fit to the observed  $K_{eq}$  values at different temperatures). The two methods may yield significantly different values for the temperature dependence of  $K_{eq}$ , but as the entropies of ClO and Cl<sub>2</sub>O<sub>2</sub> are reasonably well constrained by available spectroscopic data, third law analysis is the preferred method (Nickolaissen et al., 1994). The JPL 2002 recommendation for  $K_{eq}$  is based on third law analysis of the laboratory data given by Cox and Hayman (1988) and Nickolaissen et al. (1994) using for Cl<sub>2</sub>O<sub>2</sub>  $S^\circ(300\text{K})=302.2\text{ J K}^{-1}\text{ mol}^{-1}$  to obtain the value of  $RT/N_A \exp(\Delta_r S^\circ / R)$ , the so-called pre-exponential factor.

20 Here, standard entropies  $S^\circ$  for ClO and Cl<sub>2</sub>O<sub>2</sub> and the standard enthalpy of formation  $\Delta_f H^\circ$  for ClO are determined using statistical thermodynamics as described in Chase (1998). The uncertainty in these parameters for ClO is small with  $S^\circ(298.15\text{ K})=225.07\pm0.5\text{ J K}^{-1}\text{ mol}^{-1}$  and  $\Delta_f H^\circ(298.15\text{ K})=101.63\pm0.1\text{ kJ mol}^{-1}$ . When computing  $S^\circ$  for Cl<sub>2</sub>O<sub>2</sub> a larger uncertainty arises, because some of the vibrational frequencies used in the calculation are not exactly known. Using the frequencies

7909

and uncertainties given in Table 1 results in  $S^\circ(298.15\text{ K})=302.08^{+1.11}_{-0.42}\text{ J K}^{-1}\text{ mol}^{-1}$ . The temperature dependence of  $\Delta_f H^\circ$  for Cl<sub>2</sub>O<sub>2</sub>,  $d(\Delta_f H^\circ)/dT$ , may also be calculated from statistical thermodynamics with a relatively small uncertainty (using the same vibrational frequencies as for computing  $S^\circ$ ). If we express  $\Delta_r H^\circ$  as the sum of  $\Delta_r H^\circ(0\text{ K})$  and a temperature dependent thermal correction, Eq. (2) becomes

$$\begin{aligned} K_{eq}(T) &= \frac{RT}{N_A} e^{\Delta_r S^\circ / R} e^{-\left(\Delta_r H^\circ(0\text{ K}) + \int_{0\text{ K}}^T d(\Delta_r H^\circ)/dT\right)/RT} \\ &= \frac{RT}{N_A} e^{\Delta_r S^\circ / R} e^{-\left(\int_{0\text{ K}}^T d(\Delta_r H^\circ)/dT\right)/RT} e^{-\Delta_r H^\circ(0\text{ K})/RT} \end{aligned} \quad (3)$$

All quantities in Eq. (3) are either constant or can be calculated from statistical thermodynamics except for  $\Delta_r H^\circ(0\text{ K})$ , which can be taken from direct laboratory measurements or deduced from laboratory measurements of  $K_{eq}$  at different temperatures by a logarithmic fit, corresponding to third law analysis but taking into account the temperature dependence of  $\Delta_r H^\circ$  and  $\Delta_r S^\circ$ . The major uncertainty in this calculation arises from the uncertainties in the vibrational frequencies of Cl<sub>2</sub>O<sub>2</sub> (Table 1). However, this results in less than 0.2 kJ mol<sup>-1</sup> error in the calculated  $\Delta_r H^\circ(0\text{ K})$  values and less than 10% error in  $K_{eq}$  below 300 K.

15 Figure 1a shows various laboratory measurements of  $K_{eq}$  at different temperatures, and the temperature dependence resulting from the analysis of these data described above. Also included is the temperature dependence deduced from  $\Delta_r H^\circ$  measured by Plenge et al. (2005) and the recommendation and uncertainty given in JPL 2002. A comparison with  $K_{eq}$  deduced from stratospheric observations is shown in Fig. 1b. 20 The values obtained for  $\Delta_r H^\circ(0\text{ K})$  from the temperature dependent third law analysis of the laboratory data shown in Fig. 1a are given in Table 2, together with other values found in the literature. While three laboratory studies (Basco and Hunt, 1979; Cox and Hayman, 1988; Ellermann et al., 1995) are in excellent agreement, the values obtained by Nickolaissen et al. (1994) are significantly higher. We note three arguments 25 that support the former three studies:

1. Cox and Hayman (1988) and Basco and Hunt (1979) actually establish the equilibrium between ClO and Cl<sub>2</sub>O<sub>2</sub> while Nickolaissen et al. (1994) determine  $K_{\text{eq}}$  from measured values of  $k_{\text{rec}}$  and  $k_{\text{diss}}$  that are somewhat dependent on each other,
  2. in Nickolaissen et al. (1994) the Cl<sub>2</sub>O<sub>2</sub> entropies obtained by second and third law analyses disagree beyond the error margins of both methods, and
  3.  $K_{\text{eq}}$  resulting from the Cox and Hayman (1988) data is in excellent agreement with atmospheric measurements (Fig. 1b). At stratospheric temperatures, it corresponds almost exactly to the function inferred from aircraft observations of ClO inside the Arctic polar vortex by Avallone and Toohey (2001), which represents an upper limit to  $K_{\text{eq}}$  because their assumption of full chlorine activation means that they used maximum possible values for [Cl<sub>2</sub>O<sub>2</sub>]. Stimpfle et al. (2004) could best reproduce their simultaneous observations of ClO and Cl<sub>2</sub>O<sub>2</sub> in darkness using the Cox and Hayman (1998) value for  $K_{\text{eq}}$ , which is further supported by a number of night-time ClO measurements (Berthet et al., 2005; Glatthor et al., 2004; Pierson et al., 1999; von Clarmann et al., 1997). Observations of ClO and Cl<sub>2</sub>O<sub>2</sub> presented in von Hobe et al. (2005) suggest a value for  $K_{\text{eq}}$  even lower by a factor of 2 to 4, but equilibrium may not have been established considering lower rates of Cl<sub>2</sub>O<sub>2</sub> formation than assumed in their study (cf. Sect. 4) and their Cl<sub>2</sub>O<sub>2</sub> measurements may be biased low (cf. Sect. 5).
- Table 3 gives an overview of  $K_{\text{eq}}$  values given in the literature. While the upper (Nickolaissen et al., 1994) and lower (von Hobe et al., 2005) limits at stratospheric temperatures differ by a factor of 9 at 200 K, the values given by Plenge et al. (2005) and Avallone and Toohey (2001) and deduced here for the laboratory data of Cox and Hayman (1988) lie only 30% apart and are consistent with most observations (e.g. Glatthor et al., 2004; Stimpfle et al., 2004; Berthet et al., 2005; and, within error limits, even von Hobe et al., 2005).

7911

### 3 The Cl<sub>2</sub>O<sub>2</sub> dissociation rate constant $k_{\text{diss}}$

Low pressure rate constants for unimolecular decomposition reactions such as the reverse of Reaction (R1) may be described by the following formalism (Troe, 1977a; Troe, 1977b; Troe, 1979; Patrick and Golden, 1983):

$$k_{\text{diss},0} = \beta_c k_{\text{diss},0}^{\text{sc}} = \beta_c Z_{\text{LJ}} [\rho_{\text{vib},h}(E_0) RT / Q_{\text{vib}}] e^{-E_0/RT} F_{\text{anh}} F_E F_{\text{rot}} F_{\text{rot int}} F_{\text{corr}} \quad (4)$$

The hypothetical strong collision rate constant  $k_{\text{diss},0}^{\text{sc}}$  forms an upper limit, which is multiplied by a collision efficiency term  $\beta_c$  to take weak collision effects into account.  $Z_{\text{LJ}}$  is the Lennard-Jones collision frequency,  $\rho_{\text{vib},h}(E_0)$  the harmonic oscillator density of states,  $Q_{\text{vib}}$  the vibrational partition function,  $E_0 \cong \Delta_r H^\circ(0\text{ K})$  the reaction threshold energy (note that in Table 2,  $\Delta_r H^\circ$  values are given for the forward direction of Reaction (R1), so the sign has to be reversed here),  $F_{\text{anh}}$  the anharmonicity correction,  $F_E$  the energy dependence of the density of states and  $F_{\text{rot}}$  the external rotational contribution. The correction factor for internal rotation,  $F_{\text{rot int}}$ , is not considered here because internal rotors are not significant at low temperatures for these calculations (Patrick and Golden, 1983). Following Troe (1977b) we neglect the final factor  $F_{\text{corr}}$  introduced to correct for the coupling between the various factors and the approximations made in the calculation. A summary of the parameters in Eq. (4) and their uncertainties at various temperatures is given in Table 4. The exact calculation is described in detail by Troe (1977a, b). As for  $K_{\text{eq}}$ , the uncertainties arising from the vibrational frequencies of Cl<sub>2</sub>O<sub>2</sub> are small (<7% error for  $k_{\text{diss},0}^{\text{sc}}$ ) because the temperature dependence is determined mainly by  $E_0$  and the effects of using different vibrational frequencies on  $\rho_{\text{vib},h}(E_0)$  and  $Q_{\text{vib}}$  partially cancel.

In Fig. 2,  $k_{\text{diss},0}$  from Eq. (4) is plotted as a function of temperature and compared to laboratory studies. Using  $\Delta_r H^\circ(0\text{ K})$  from Plenge et al. (2005) and  $\beta_c(300\text{ K})=0.6$ , the theoretical value derived here is in excellent agreement with laboratory data between 242 and 261 K recently published by Bröske and Zabel (2006). Here, we only shown data obtained at pressures below 10 mbar, where falloff behavior is assumed to be

7912

negligible (cf. Sect. 4). The values of  $k_{\text{diss},0}$  derived in the Nickolaisen et al. (1994) study fall significantly below even the lowest theoretical value using  $\Delta_r H^\circ$  (0 K) derived from Cox and Hayman (1988) and  $\beta_c$  (300 K)=0.3. Bröske and Zabel (2006) prepared  $\text{Cl}_2\text{O}_2$  and monitored its loss whereas Nickolaisen et al. (1994) obtained  $k_{\text{diss}}$  from fitting the observed decay of ClO in the temperature range 260–310 K to an overall reaction mechanism. We feel that the potential sources of error in the method employed by Bröske and Zabel (2006) are smaller, because the data are much easier to interpret and the only other loss mechanism for  $\text{Cl}_2\text{O}_2$  in this experiment are wall effects that were not apparent over the pressure range used (Bröske and Zabel, 2006).

Bröske and Zabel (2006) compare their results to theoretical predictions of the low pressure rate constant using the formalism by Troe (1977a, b) described above (Eq. 4). Choosing  $\beta_c$  (250 K)=0.3, they derive  $\Delta_r H^\circ$  (0 K)=66.4±3.0 kJ mol<sup>-1</sup> which is lower than the laboratory values presented in Table 2 and would imply an equilibrium constant similar to von Hobe et al. (2005). On the other hand Bröske and Zabel (2006) obtain  $K_{\text{eq}}$  between Cox and Hayman (1988) and Plenge et al. (2005) when multiplying  $k_{\text{diss},0}$  with  $k_{\text{rec},0}$  recommended by JPL 2002. If the laboratory measurements of Bröske and Zabel (2006) are correct, this would imply that the values recommended for  $K_{\text{eq}}$  and  $k_{\text{rec},0}$  by JPL 2002 are inconsistent (cf. Sect. 4).

Because of the limited temperature range over which Bröske and Zabel (2006) conducted their experiment, the uncertainty of their fit to the data becomes rather large at temperatures well below or above 242–261 K. Therefore we fit a simple exponential function to  $k_{\text{diss},0}$  from Eq. (4) with  $\Delta_r H^\circ$  (0 K) from Plenge et al. (2005) and  $\beta_c$  (300 K)=0.6 that best fits the Bröske and Zabel (2006) measurements:

$$k_{\text{diss},0} = 1.66 \times 10^{-6} \text{e}^{-7821/T} \quad (5)$$

7913

#### 4 The $\text{Cl}_2\text{O}_2$ formation rate constant $k_{\text{rec}}$

The  $\text{Cl}_2\text{O}_2$  formation rate constant  $k_{\text{rec}}$  has been determined in a number of laboratory studies employing flash photolysis with time resolved UV absorption spectroscopy (Sander et al., 1989; Trolier et al., 1990; Nickolaisen et al., 1994; Bloss et al., 2001; Boakes et al., 2005). Except for the most recent investigation (Boakes et al., 2005), the values given for the low pressure limit  $k_{\text{rec},0}$  at temperatures above about 240 K agree well, but at stratospheric temperatures between 180 and 220 K there is a large discrepancy (Fig. 3).

Using Eq. (1),  $k_{\text{rec},0}$  can be calculated by multiplying  $K_{\text{eq}}$  obtained from Eq. (3) and  $k_{\text{diss},0}$  from Eq. (4). As long as the choice of  $\Delta_r H^\circ$  (0 K) is consistent, the  $\text{e}^{-\Delta_r H^\circ(0\text{K})/RT}$  and  $\text{e}^{-E_0/RT}$  terms in Eqs. (3) and (4) cancel, and the remaining dependency on  $E_0$  and hence on the choice of the equilibrium constant is small. The following expression is obtained:

$$k_{\text{rec},0} = \frac{R^2 T^2}{N_A} \beta_c \rho_{\text{vib},h} Z_{\text{LJ}} \frac{1}{Q_{\text{vib}}} F_{\text{anh}} F_{\text{E}} F_{\text{rot}} \text{e}^{\Delta_r S^\circ/R} \text{e}^{-\left(\int_{0\text{K}}^T d\Delta_r H^\circ/dT\right)/RT} \quad (6)$$

$R$ ,  $N_A$ ,  $\rho_{\text{vib},h}$  and  $F_{\text{anh}}$  are independent of temperature. The temperature dependence of the remaining terms is calculated or fitted over the temperature range 170 to 320 K to the functional form  $T^n$ , giving  $T^{-1.5 \pm 0.3}$  for  $1/Q_{\text{vib}}$ ,  $T^{-1.1 \pm 0.1}$  for  $F_{\text{rot}}$ ,  $T^{-0.9 \pm 0.4}$  for  $\text{e}^{\Delta_r S^\circ/R}$ ,  $T^{-1.2 \pm 0.2}$  for  $\text{e}^{-\left(\int_{0\text{K}}^T d\Delta_r H^\circ/dT\right)/RT}$  and  $T^{0.2 \pm 0.1}$  for  $\beta_c Z_{\text{LJ}} F_{\text{E}}$  combined (the individual temperature dependence of these three terms is complicated but small, cf. Table 4). The uncertainties in the exponents incorporate uncertainties of the parameters used (e.g. vibrational frequencies) as well as uncertainties from the fits, in some cases taking the extremes at either end of the temperature range as upper and lower limits. Together with the  $T^2$  term, this yields an overall temperature dependence of  $T^{-2.9 \pm 0.6}$  for  $k_{\text{rec},0}$ . The uncertainty in the vibrational frequencies has a larger effect on  $k_{\text{rec},0}$  than on  $K_{\text{eq}}$  and  $k_{\text{diss},0}$  due to the sensitivity of  $\rho_{\text{vib},h}$  and  $Q_{\text{vib}}$  (Table 4) as well as  $\text{e}^{\Delta_r S^\circ/R}$  and

7914

$e^{-\left(\int_{10K}^T d\Delta_r H^\circ/dT\right)RT}$ , resulting in an error for  $k_{\text{rec},0}$  of up to 15% from the uncertainties given in Table 1.

It is evident from Fig. 3 that at stratospheric temperatures,  $k_{\text{rec},0}$  from Bloss et al. (2001) and even more so from Boakes et al. (2005) are inconsistent with  $k_{\text{rec},0}$  calculated from Eq. (5) even for  $\beta_c=1$ . The temperature dependence of  $k_{\text{rec},0}$  given in these two studies by exponents of  $-4.5$  and  $-3.8$  respectively is also inconsistent with the temperature dependence of  $k_{\text{rec},0}$  derived using Eq. (5). On the other hand, using  $\beta_c=0.6$  (most consistent with  $k_{\text{diss},0}$  observed by Bröske and Zabel (2006), cf. Sect. 3) yields a  $k_{\text{rec},0}$  corresponding almost exactly to the  $T^n$  treatment of Nickolaisen et al. (1994), which is in reasonable agreement with Sander et al. (1989) and Trolrier et al. (1990). Moreover, the temperature exponent of  $-3.01\pm0.20$  given by Nickolaisen et al. (1994) is in excellent agreement with the  $-2.9\pm0.6$  we have deduced above.

A value for  $k_{\text{rec},0}$  higher than the derived  $k_{\text{rec},0}^{\text{SC}}$  (i.e.  $\beta_c=1.0$ ) is difficult to rationalize: thermal decomposition faster than  $k_{\text{diss},0}^{\text{SC}}$  derived in Sect. 3 is unlikely on theoretical grounds (Golden, 2003) and would contradict both available laboratory studies (Bröske and Zabel, 2006; Nickolaisen et al., 1994). A significantly higher value for  $K_{\text{eq}}$  is incompatible with most field observations of ClO and Cl<sub>2</sub>O<sub>2</sub>. This is not in conflict with the notion of Bröske and Zabel (2006) that  $K_{\text{eq}}$  calculated from their  $k_{\text{diss}}$  and  $k_{\text{rec}}$  from Bloss et al. (2001) is consistent with Cox and Hayman (1988) and Plenge et al. (2005), because over the temperature range of their experiment, i.e. 242–261 K,  $k_{\text{rec}}$  from Bloss et al. (2001) and Nickolaisen et al. (1994) are equivalent (Fig. 3).

In the atmosphere somewhat lower values than the low pressure limits are usually observed for rate constants such as  $k_{\text{diss}}$  and  $k_{\text{rec}}$  due to falloff behavior with increasing pressure. Effective rate constants are estimated using the following expression (Troe,

7915

1979; Patrick and Golden, 1983):

$$k = \frac{k_0[M]}{1 + k_0[M]/k_\infty} F \left[ 1 + \left( \log \left\{ \frac{k_0[M]}{k_\infty} \right\} \right)^2 \right]^{-1} \quad (7)$$

where  $k_\infty$  is the high pressure limiting rate constant and  $F \sim 0.6$  is the broadening parameter. Parameterizations for  $k_{\text{rec},\infty}$  given in the laboratory studies mentioned above are compared in Fig. 4. The largest difference at stratospheric temperatures is about a factor of two. We choose to follow the JPL 2002 recommendation for  $k_{\text{rec},\infty}$  which provides an intermediate estimate at stratospheric temperatures with a temperature dependence of  $T^{-2.4}$ . Uncertainties in  $k_{\text{rec},\infty}$  are not as critical as the choice for  $k_{\text{rec},0}$  at stratospheric pressures. Below 150 hPa, variation of  $k_{\text{rec},\infty}$  by a factor of two changes the resulting  $k_{\text{rec}}$  by 10 % at most. Falloff behavior also applies to  $k_{\text{diss}}$ . Because no reliable measurement of  $k_{\text{diss},\infty}$  exists (Bröske and Zabel, 2006, state that the uncertainty of their proposed  $k_{\text{diss},\infty}$  is large because measurements were only made at low pressures), it is calculated from  $k_{\text{rec},\infty}$  through  $K_{\text{eq}}$ .

## 5 The Cl<sub>2</sub>O<sub>2</sub> absorption cross section $\sigma_{\text{ClOOCi}}$ and photolysis frequency $J$

Of all parameters governing ozone loss by the ClO dimer catalytic cycle, the photolysis frequency  $J$  based on the absorption cross section  $\sigma_{\text{ClOOCi}}$  holds the greatest uncertainty. It has been determined in a number of laboratory studies (Basco and Hunt, 1979; Molina and Molina, 1987; Permien et al., 1988; Cox and Hayman, 1988; DeMore and Tschuikow-Roux, 1990; Burkholder et al., 1990; Huder and DeMore, 1995; Pope et al., 2005). The spectra obtained by Basco and Hunt (1979) and Molina and Molina (1987) are significantly different in shape from the other studies and have been proposed to be influenced by Cl<sub>2</sub>O<sub>3</sub> and possibly other impurities. The other studies agree extremely well in the peak region around 245 nm, but disagree by up to a factor of five at higher wavelength controlling  $J$  in the atmosphere (Fig. 5). The JPL 2002 recommendation

7916

for  $\sigma_{\text{ClOOCl}}$  also shown in Fig. 5 is based on an average of the values reported by Per-  
mien et al. (1988), Cox and Hayman (1988), DeMore and Tschuikow-Roux (1990) and  
Burkholder et al. (1990).

In the analysis of the field data below, we also test a slightly modified wavelength  
dependent average of reported cross sections named “MPIC” (Tables 5 and 6) that  
falls between JPL 2002 and Burkholder et al. (1990) (Fig. 5). As stated in Table 5,  
the MPIC cross sections listed in Table 6 are derived in the 302–360 nm range (which  
strongly affects the resulting  $J$  and forms the basis for the log-linear extrapolation to  
higher wavelengths) from averaging the data from Burkholder et al. (1990) and DeMore  
and Tschuikow-Roux (1990). In this wavelength range, the MPIC averaged values do  
not consider the much lower data set obtained by Huder and DeMore (1995), because  
it is believed that not enough experimental information was provided to justify the use of  
this cross section above 310 nm. For wavelengths greater than 310 nm, the Huder and  
DeMore (1995) cross section is based on a log-linear extrapolation of data obtained at  
shorter wavelengths. However, it should be noted that the most recent study by Pope  
et al. (2005) suggests cross sections roughly equivalent to Huder and DeMore (1995)  
out to  $\sim 350$  nm, and possibly considerably lower values than the by Huder and DeMore  
(1995) cross sections for the atmospherically important region of wavelengths longer  
than 350 nm.

Photolysis frequencies of  $\text{Cl}_2\text{O}_2$  are obtained by multiplying the absorption cross sec-  
tion by the actinic flux and integrating over all atmospherically relevant wavelengths.  
Here we use a full radiative model that takes into account solar zenith angle (SZA),  
ambient pressure, overhead ozone and albedo (Salawitch et al., 1994). This is the  
same radiative transfer model used by Stimpfle et al. (2004) to examine the SOLVE  
observations of ClO and ClOOCl. Variations in albedo along the flight track of the ER-2  
and Geophysica aircraft are obtained primarily from TOMS reflectivity maps. However,  
measurements from a UV/Vis spectrometer aboard the ER-2 are used when these data  
are available (Stimpfle et al., 2004). The ozone profiles used to constrain the radiative  
model are obtained primarily from an assimilation of satellite profiles scaled to match

7917

total ozone column measured by TOMS along the flight track. However, partial ozone  
columns from the UV/Vis spectrometer are used for some portions of the ER-2 simula-  
tions, when these data are available (Stimpfle et al., 2004). Under typical stratospheric  
conditions,  $J$  values based on the cross sections by Burkholder et al. (1990) and Huder  
and DeMore (1995) differ by a factor of about 2.5. Values based on JPL 2002 and MPIC  
lie between the two. The variation in  $J$  due to the various cross sections is much larger  
than typical differences due to reasonable uncertainties in overhead ozone and albedo.

### 5.1 Photochemical steady state analysis of field data

As described by Avallone and Toohey (2001), effective atmospheric  $J$  values can be  
estimated from atmospheric observations assuming photochemical steady state:

$$J = k_{\text{rec}} \left( \frac{[\text{ClO}]^2[\text{M}]}{[\text{Cl}_2\text{O}_2]} - \frac{[\text{M}]}{K_{\text{eq}}} \right) \quad (8)$$

The resulting  $J$  values depend critically on the choice of  $k_{\text{rec}}$ . We utilize the second  
order rate constant from Eq. (7) (that replaces the  $k_{\text{rec}}[\text{M}]$  term in Eq. 8) with  $k_{\text{rec},0}$  from  
Nickolaisen et al. (1994) and  $k_{\text{rec},\infty}$  from JPL 2002, which have been reasonably well  
constrained in Sect. 4.  $K_{\text{eq}}$  is calculated according to Plenge et al. (2005) (cf. Sect. 2).  
This choice is critical at high solar zenith angles where the contribution from thermal  
dissociation to the overall rate of  $\text{Cl}_2\text{O}_2$  removal becomes significant.

Equation (8) only yields reliable  $J$  values when the steady state assumption holds.  
To test this, we employ a time dependent diurnal box model containing the relevant  
photochemical reactions that govern the partitioning of active chlorine and bromine  
in the perturbed polar vortex (Canty et al., 2005). We compare  $J$  derived from the  
simulated abundances of ClO and  $\text{Cl}_2\text{O}_2$  using Eq. (8) to the values of  $J$  used in the  
photochemical model, which are based on radiative transfer calculations. The results  
shown in Fig. 6 indicate that the steady state assumption is valid at SZA  $< 84^\circ$ , but  
significant deviations exist at higher SZA. During early morning,  $\text{Cl}_2\text{O}_2$  accumulated

7918

during the night needs time to photolyse until steady state is reached, and  $J$  from Eq. (8) falls below  $J$  calculated by the radiative model. During late evening,  $\text{Cl}_2\text{O}_2$  needs time to reform causing  $J$  from Eq. (8) to lie above the radiative  $J$ . The difference between  $J$  found using Eq. (8) and the radiative  $J$  is larger at lower temperatures, because of the temperature effect on  $k_{\text{rec}}$  and  $K_{\text{eq}}$ . For larger cross sections that lead to faster photolysis (i.e., Burkholder et al., 1990), the relative difference between the two values of  $J$  is slightly smaller than for smaller cross sections that lead to slower photolysis (i.e., Huder and DeMore, 1995). For air parcels that reach SZA of  $\sim 84$  to  $90^\circ$  at noon, the difference between  $J$  found using Eq. (8) and radiative  $J$  is smaller than results shown in Fig. 6. Under these conditions, air masses spend more time at high SZA, resulting in chemical evolution that is close to instantaneous steady state. Equation (8) will yield reliable results provided the data analysis is focused on SZA  $< 84^\circ$ .

In Fig. 7,  $J$  values estimated from observations of  $[\text{ClO}]$  and  $[\text{Cl}_2\text{O}_2]$  made during field campaigns in several Arctic winters (SOLVE, 1999/2000: Stimpfle et al., 2004; EUPLEX and ENVISAT Arctic Validation, 2002/3: von Hobe et al., 2005; Arctic Vortex flight 2005: von Hobe et al., 2006) using Eq. (8) are plotted as a function of SZA. Error bars are based on relative errors for  $[\text{ClO}]$  (squared) and  $[\text{Cl}_2\text{O}_2]$  that propagate into the relative error for  $J$ . The effect can be rather large, especially at low concentrations where the relative measurement error is usually larger. At high zenith angles  $\text{Cl}_2\text{O}_2$  thermal dissociation becomes comparable to photolysis and  $[\text{ClO}]^2/[\text{Cl}_2\text{O}_2]$  approaches  $1/K_{\text{eq}}$ , resulting in a large relative error for the difference and hence  $J$ . Also shown in Fig. 7 are  $J$  values based on the radiative model for the different cross sections given by Burkholder et al. (1990), Huder and DeMore (1995), JPL 2002 and MPIC. Variations along the aircraft flight track of overhead ozone, albedo, and pressure cause the radiative  $J$  values to vary in a manner that is not monotonic with SZA. The error bars on Fig. 7 for radiative  $J$  represent the maximum and minimum values for  $2^\circ$  wide SZA bins.

7919

A large number of data points, particularly from the SOLVE data (Stimpfle et al., 2004), follow a dependence on SZA very similar to  $J_{\text{MPIC}}$ ,  $J_{\text{JPL02}}$  and  $J_{\text{Burkholder}}$ . However, numerous points diverge from the compact relationship with SZA, especially at high SZA. Partly, these deviations can be explained by the non-steady state effects described above. In the bottom panel of Fig. 7, data are marked according to the time of day when the measurement was made. At SZA  $> 85^\circ$ , the SOLVE data cluster around two separate lines, the higher one containing almost all points measured in the evening. This is consistent with expectation, as shown in Fig. 6.

Even though all flights carried out during the ENVISAT Arctic Validation Campaign were carried out in the morning and hence are expected to fall below the steady state curve, and most EUPLEX flights were evening flights expected to fall above, for the data from these two campaigns the discrepancy is often too large to be explained by non steady state effects alone. As observed in the empirical fit used to obtain  $K_{\text{eq}}$  from nighttime measurements (von Hobe et al., 2005),  $[\text{Cl}_2\text{O}_2]/[\text{ClO}]^2$  ratios observed during the EUPLEX campaign are considerably lower than during other field campaigns, which via Eq. (8) translates into faster photolysis rates. For many data points the discrepancy lies within the error bounds of the data, but the reason for this obvious underestimation of  $[\text{Cl}_2\text{O}_2]/[\text{ClO}]^2$  on the order of  $\sim 40\%$  is unresolved. Indeed, it is unclear why the EUPLEX measurements of  $[\text{Cl}_2\text{O}_2]/[\text{ClO}]^2$  can differ substantially even compared to other measurements by the same instrument. As mentioned above, a 40% relative error on  $[\text{Cl}_2\text{O}_2]/[\text{ClO}]^2$  can produce a much larger relative error for  $J$  derived from Eq. (8) at high zenith angles often encountered during EUPLEX. A source of error leading to an underestimation of  $J$  may be present in the data from the ENVISAT Validation campaign. Von Hobe et al. (2005) state that contribution from  $\text{ClONO}_2$  at the dimer dissociation temperature in their measurement is less than 1%. However, at the end of the winter after significant deactivation and hence high  $\text{ClONO}_2$  and moderate to low levels of active chlorine, this may introduce a significant error in the measurement of  $\text{Cl}_2\text{O}_2$ .

7920



For the SOLVE data and the Vortex 2005 flight, the ratio  $J_{\text{Eq. (8)}}/J_{\text{radiative}}$  is plotted as a function of solar zenith angle (SZA) in Fig. 8. As described above, the steady state assumption does not hold at SZA >84°, and the uncertainties can be ascribed to non-steady state effects. Below 84°, uncertainties in  $J$  inferred from Eq. (8) still exist, and  $J$  cannot be deduced conclusively from the observations used. However, it can be said that the best agreement is achieved for the JPL 2002 and the MPIC cross sections, while the cross sections presented by Huder and DeMore (1995) are clearly inconsistent with the atmospheric observations.

Avallone and Toohey (2001) presented a steady state analysis of ClO observations during the AASE field campaigns in the Arctic vortex during the winters 1988/89 and 1991/92. In contrast to the results presented here, their steady state  $J$  values support the cross section measurements by Huder and DeMore (1995). However, they used Cl<sub>2</sub>O<sub>2</sub> concentrations based on the assumption that all available inorganic chlorine is activated and in the form of either ClO or Cl<sub>2</sub>O<sub>2</sub> (cf. Sect. 2), thus representing an upper limit for [Cl<sub>2</sub>O<sub>2</sub>] resulting via Eq. (8) in a lower limit for  $J$ . Deviations from their assumption will have a larger impact on their  $J$  value than on their  $K_{\text{eq}}$  because the relative change of [Cl<sub>2</sub>O<sub>2</sub>] would be greater at lower concentrations during the day.

## 5.2 Box model studies

The results of the photochemical steady state analysis are in good agreement with the results from the comparison of the SOLVE data with box model studies by Stimpfle et al. (2004), where  $J_{\text{JPL02}}$  was too small and  $J_{\text{Burkholder}}$  was too large when using  $k_{\text{rec},0}$  from JPL 2000 (Sander et al., 2000), which is basically the same as  $k_{\text{rec},0}$  from Nickolaisen et al. (1994).

We also carried out a box model study similar to Stimpfle et al. (2004) to provide a further test independent of any non-steady-state-effects. Observations were taken from the Arctic vortex 2005 flight (von Hobe et al., 2006). These are probably the most reliable HALOX measurements due to high ClO<sub>x</sub> and low ClONO<sub>2</sub> levels and stronger chlorine emission lamps than were available in the 2002/03 winter (lamp out-

7921

put strongly influences sensitivity of the chemical conversion reference fluorescence technique used by HALOX). Due to the wide range of solar zenith angles encountered, the flight is also most suitable to constrain  $J$ . Simulations were carried out using CLaMS (= Chemical Lagrangian Model of the Stratosphere, McKenna et al., 2002) along back trajectories from ECMWF wind fields initialized at 04:00 a.m. UTC on the flight day with [ClO<sub>x</sub>] = [ClO]<sub>obs</sub> + 2[Cl<sub>2</sub>O<sub>2</sub>]<sub>obs</sub> distributed between ClO and Cl<sub>2</sub>O<sub>2</sub> using  $K_{\text{eq}}$  from Plenge et al. 2005), which was also used by the model together with  $k_{\text{rec},0}$  from Nickolaisen et al. (1994) and  $k_{\text{rec},\infty}$  from JPL 2002. Four model runs using different parameterizations for  $\sigma_{\text{ClOOCl}}$  were carried out (Fig. 9). In agreement with the steady state analysis presented in Sect. 5.1, the results using  $\sigma_{\text{ClOOCl}}$  from Huder and DeMore (1995) are mostly outside the error margins, and on average, the best fit is obtained with the MPIC and the Burkholder et al. (1990) cross sections.

## 6 Conclusions

At stratospheric temperatures, similar values for  $K_{\text{eq}}$  are obtained from the parameterizations given by Avallone and Toohey (2001), Cox and Hayman (1988) and Plenge et al. (2005), which all fulfill the theoretical constraints presented here and are in good agreement with atmospheric observations. The temperature dependence of both  $\Delta_r S^\circ$  and  $\Delta_r H^\circ$  has to be taken into account in order to extrapolate  $K_{\text{eq}}$  over a large temperature range, to obtain exact values for  $\Delta_r H^\circ$  (0 K), and to derive the temperature dependence of  $k_{\text{diss}}$  and  $k_{\text{rec}}$  as described above. However, for stratospheric conditions, a more complex expression for the temperature dependence of  $K_{\text{eq}}$  than given by JPL 2002 may not be necessary, especially in light of the significant differences in estimates of  $K_{\text{eq}}$  from various laboratory groups.

A parameterization for the low pressure unimolecular dissociation rate constant  $k_{\text{diss},0}$  of Cl<sub>2</sub>O<sub>2</sub> is given in Eq. (5), which provides a useful extrapolation of the laboratory measurement by Bröske and Zabel (2006). As noted in Sect. 4, falloff behavior applies to this reaction, so at atmospheric pressures  $k_{\text{diss}}$  should be calculated from

$K_{\text{eq}}$  and the falloff expression for  $k_{\text{rec}}$  (Eq. 7).

Magnitude and temperature dependence of the low pressure limiting ClO recombination rate constant  $k_{\text{rec},0}$  given by Nikolaisen et al. (1994) are in excellent agreement with values derived from  $K_{\text{eq}}$  and  $k_{\text{diss},0}$ . The choice of the high pressure limit  $k_{\text{rec},\infty}$  is not critical at stratospheric pressures and the least potential error is introduced by using the intermediate value recommended by JPL 2002. A small downward correction of 6% may be applied to take account of the lower efficiency of atmospheric  $\text{O}_2$  as a third body compared to  $\text{N}_2$  (Bloss et al., 2001).

Using these kinetic parameters in a simple steady state analysis and in box model studies, atmospheric observations of ClO and  $\text{Cl}_2\text{O}_2$  appear to be best explained using  $J$  values derived from the MPIC  $\text{Cl}_2\text{O}_2$  absorption cross sections. However, the scatter of the data is large and within the uncertainties the JPL 2002 cross sections and those suggested by Burkholder et al. (1990) still give a consistent picture for most of the data. Results of the analysis of  $J$  values presented here are in excellent agreement with Stimpfle et al. (2004). The cross sections measured by Huder and DeMore (1995) are clearly too low to be consistent with nearly all atmospheric observations, including earlier studies of ClO in the Antarctic vortex (Shindell and de Zafra, 1995; Shindell and de Zafra, 1996; Solomon et al., 2002). If these cross sections or the even lower values recently presented by Pope et al. (2005) are correct, then either some unidentified loss process converts  $\text{Cl}_2\text{O}_2$  to ClO in the polar vortex, or the formation of  $\text{Cl}_2\text{O}_2$  from ClO proceeds much slower than even the lowest rates reported based on laboratory studies, or [ClO] in the polar vortices is overestimated in nearly all available observations.

The kinetic parameters suggested here, i.e.  $K_{\text{eq}}$  from Avallone and Toohey (2001), Cox and Hayman (1988) and Plenge et al. (2005),  $k_{\text{diss},0}$  measured by Bröske and Zabel (2006) and extrapolated using unimolecular rate theory (Troe, 1979; Patrick and Golden, 1983),  $k_{\text{rec},0}$  and  $k_{\text{rec},\infty}$  given by Nikolaisen et al. (1994) and JPL 2002 respectively, and  $J$  derived from  $\sigma_{\text{ClOOCi}}$  approximately halfway between the JPL 2002 evaluation and Burkholder (1990), termed here MPIC, are consistent internally and with stratospheric observations of chlorine oxides. Provided that there are no large errors in

7923

these laboratory studies that eliminate each other in the calculations presented in this study, and that there is no fundamental problem with the field measurement techniques for ClO and  $\text{Cl}_2\text{O}_2$ , we seem to have reached good understanding of the kinetics of the ClO dimer catalytic cycle as given by Reactions (R1) to (R4). However, given the large discrepancies with some other laboratory studies mentioned above, some open questions remain. For example, it is important to identify the processes causing faster loss of ClO in the laboratory studies by Bloss et al. (2001) and Boakes et al. (2005), because it cannot be excluded that these processes play a role in the atmosphere under certain conditions. An enhancement of the ClO recombination rate due to a chaperone mechanism in the presence of  $\text{Cl}_2$  has been suggested by Nikolaisen et al. (1994). Similar effects due to other molecules or even heterogeneous processes cannot be ruled out. The possibility of pressure and temperature dependent formation of other  $\text{Cl}_2\text{O}_2$  isomers than ClOOCi has been proposed in several studies (Bloss et al., 2001; Boakes et al., 2005; Bröske and Zabel, 2006; Golden, 2003; Nikolaisen et al., 1994; von Hobe et al., 2005). Finally there may be yet unidentified reactions involving ClO and  $\text{Cl}_2\text{O}_2$ .

*Acknowledgements.* We thank MDB for their support and supply of avionic data during the Geophysica field campaigns, which were funded by the EU within the VINTERSOL-EUPLEX and APE-INFRA projects and by ESA and DLR in the context of ENVISAT Validation activities. We gratefully acknowledge R. Stimpfle for providing the ClO and  $\text{Cl}_2\text{O}_2$  measurements conducted during the ER-2 SOLVE campaign in winter 1999/2000, and ECMWF for providing meteorological analyses.

## References

- Avallone, L. M. and Toohey, D. W.: Tests of halogen photochemistry using in situ measurements of ClO and BrO in the lower polar stratosphere, *J. Geophys. Res.*, 106(D10), 10 411–10 421, 2001.
- Basco, N. and Hunt, J. E.: Mutual Combination of ClO Radicals, *Int. J. Chem. Kin.*, 11(6), 649–664, 1979.

7924

- Berthet, G., Ricaud, P., Lefevre, F., Le Flochmoen, E., Urban, J., Barret, B., Lautie, N., Dupuy, E., De la Noe, J., and Murtagh, D.: Nighttime chlorine monoxide observations by the Odin satellite and implications for the ClO/Cl<sub>2</sub>O<sub>2</sub> equilibrium, *Geophys. Res. Lett.*, 32(11), L11812, doi:10.1029/2005GL022649, 2005.
- 5 Birk, M., Friedl, R. R., Cohen, E. A., Pickett, H. M., and Sander, S. P.: The Rotational Spectrum and Structure of Chlorine Peroxide, *J. Chem. Phys.*, 91(11), 6588–6597, 1989.
- Bloss, W. J., Nickolaissen, S. L., Salawitch, R. J., Friedl, R. R., and Sander, S. P.: Kinetics of the ClO self-reaction and 210 nm absorption cross section of the ClO dimer, *J. Phys. Chem.*, 105(50), 11 226–11 239, 2001.
- 10 Boakes, G., Mok, W. H. H., and Rowley, D. M.: Kinetic studies of the ClO plus ClO association reaction as a function of temperature and pressure, *Phys. Chem. Chem. Phys.*, 7(24), 4102–4113, 2005.
- Bröske, R. and Zabel, F.: Thermal decomposition of ClOOCl, *J. Phys. Chem.*, 110(9), 3280–3288, 2006.
- 15 Burkholder, J. B., Orlando, J. J. and Howard, C. J.: Ultraviolet-Absorption Cross-Sections of Cl<sub>2</sub>O<sub>2</sub> between 210 and 410 nm, *J. Phys. Chem.*, 94(2), 687–695, 1990.
- Canty, T., E. D. Rivière, R. J. Salawitch, G. Berthet, J.-B. Renard, K. Pfeilsticker, M. Dorf, A. Butz, H. Bösch, R. M. Stimpfle, D. M. Wilmouth, E. C. Richard, D. W. Fahey, P. J. Popp, M. R. Schoeberl, L. R. Lait, and T. P. Bui, Nighttime OCIO in the winter Arctic vortex, *J. Geophys. Res.*, 110, D01301, doi:10.1029/2004JD005035, 2005.
- 20 Chase, M. W.: NIST-JANAF thermochemical tables, *J. Phys. Chem. Ref. Data Monogr.*, 9, 1, 1998.
- Cheng, B. M. and Lee, Y. P.: Production and Trapping of Gaseous Dimeric ClO – the Infrared-Spectrum of Chlorine Peroxide (ClOOCl) in Solid Argon, *Journal. Chem. Phys.*, 90(11), 5930–5935, 1989.
- 25 Cox, R. A. and Hayman, G. D.: The Stability and Photochemistry of Dimers of the ClO Radical and Implications For Antarctic Ozone Depletion, *Nature*, 332(6167), 796–800, 1988.
- DeMore, W. B. and Tschuikow-Roux, E.: Ultraviolet-Spectrum and Chemical-Reactivity of the ClO Dimer, *J. Phys. Chem.*, 94(15), 5856–5860, 1990.
- 30 Ellermann, T., Johnsson, K., Lund, A. and Pagsberg, P.: Kinetics and Equilibrium-Constant of the Reversible-Reaction ClO+ClO+M-Reversible-Arrow-Cl<sub>2</sub>O<sub>2</sub>+M at 295-K, *Acta Chem. Scand.*, 49(1), 28–35, 1995.
- Glatthor, N., von Clarmann, T., Fischer, H., Funke, B., Grabowski, U., Höpfner, M., Kellmann,

7925

- S., Kiefer, M., Linden, A., Milz, M., Steck, T., Stiller, G. P., Mengistu Tsidu, G., and Wang, D.-Y.: Spaceborne ClO observations by the Michelson Interferometer for Passive Atmospheric Sounding (MIPAS) before and during the Antarctic major warming in September/October 2002, *J. Geophys. Res.*, 109(D11), doi:10.1029/2003JD004440, 2004.
- 5 Golden, D. M.: Reaction ClO + ClO → products: Modeling and parameterization for use in atmospheric models, *Int. J. Chem. Kin.*, 35(5), 206–211, 2003.
- Huder, K. J. and DeMore, W. B.: Absorption Cross-Sections of the ClO Dimer, *J. Phys. Chem.*, 99(12), 3905–3908, 1995.
- Jacobs, J., Kronberg, M., Müller, H. S. P., and Willner, H.: An Experimental-Study On the Photochemistry and Vibrational Spectroscopy of 3 Isomers of Cl<sub>2</sub>O<sub>2</sub> Isolated in Cryogenic Matrices, *J. Am. Chem. Soc.*, 116(3), 1106–1114, 1994.
- 10 Lee, T. J., Rohlffing, C. M., and Rice, J. E.: An Extensive Ab-initio Study of the Structures, Vibrational-Spectra, Quadratic Force-Fields, and Relative Energetics of 3 Isomers of Cl<sub>2</sub>O<sub>2</sub>, *J. Chem. Phys.*, 97(9), 6593–6605, 1992.
- 15 McElroy, M. B., Salawitch, R. J., Wofsy, S. C., and Logan, J. A.: Reductions of Antarctic Ozone Due to Synergistic Interactions of Chlorine and Bromine, *Nature*, 321(6072), 759–762, 1986.
- McGrath, M. P., Clemmshaw, K. C., Rowland, F. S., and Hehre, W. J.: Structures, Relative Stabilities, and Vibrational-Spectra of Isomers of Cl<sub>2</sub>O<sub>2</sub> – the Role of the Chlorine Oxide Dimer in Antarctic Ozone Depleting Mechanisms, *J. Phys. Chem.*, 94(15), 6126–6132, 1990.
- 20 McKenna, D. S., Grooß, J.-U., Gunther, G., Konopka, P., Müller, R., Carver, G., and Sasano, Y.: A new Chemical Lagrangian Model of the Stratosphere (CLaMS) – 2. Formulation of chemistry scheme and initialization, *J. Geophys. Res.*, 107(D15), 4256, doi:10.1029/2000JD000113, 2002.
- Molina, L. T. and Molina, M. J.: Production of Cl<sub>2</sub>O<sub>2</sub> from the Self-Reaction of the ClO Radical, *J. Phys. Chem.*, 91(2), 433–436, 1987.
- 25 Moore, T. A., Okumura, M., Seale, J. W., and Minton, T. K.: UV photolysis of ClOOCl, *J. Phys. Chem.*, 103(12), 1691–1695, 1999.
- Nickolaissen, S. L., Friedl, R. R., and Sander, S. P.: Kinetics and Mechanism of the ClO+ClO Reaction – Pressure and Temperature Dependences of the Bimolecular and Termolecular Channels and Thermal-Decomposition of Chlorine Peroxide, *J. Phys. Chem.*, 98(1), 155–169, 1994.
- 30 Patrick, R. and Golden, D. M.: 3rd-Order Rate Constants of Atmospheric Importance, *Int. J. Chem. Kin.*, 15(11), 1189–1227, 1983.

7926

- Permien, T., Vogt, R., and Schindler, R. N.: Mechanisms of Gas Phase-Liquid Phase Chemical Transformations, in: Air Pollution Report #17, edited by: Cox, R. A., Environmental Research Program of the CEC: Brussels, 1988.
- Pierson, J. M., McKinney, K. A., Toohey, D. W., Margitan, J., Schmidt, U., Engel, A., and Newman, P. A.: An investigation of ClO photochemistry in the chemically perturbed arctic vortex, *J. Atmos. Chem.*, 32(1), 61–81, 1999.
- Plenge, J., Flesch, R., Kühl, S., Vogel, B., Müller, R., Stroh, F., and Rühl, E.: Ultraviolet photolysis of the ClO dimer, *J. Phys. Chem.*, 108(22), 4859–4863, 2004.
- Plenge, J., Kühl, S., Vogel, B., Müller, R., Stroh, F., von Hobe, M., Flesch, R., and Rühl, E.: Bond strength of chlorine peroxide, *J. Phys. Chem.*, 109(30), 6730–6734, 2005.
- Pope, F., Hansen, J., Bayes, K., Friedl, R., and Sander, S.: Re-determination of the UV Absorption Cross Sections of ClOOCl. Eos Transactions AGU, 86(52), Fall Meet. Suppl., Abstract A13D-0970, 2005.
- Salawitch, R. J., S. C. Wofsy, P. O. Wennberg, R. C. Cohen, J. G. Anderson, D. W. Fahey, R. S. Gao, E. R. Keim, E. L. Woodbridge, R. M. Stimpfle, J. P. Koplów, D. W. Kohn, C. R. Webster, R. D. May, L. Pfister, E. W. Gottlieb, H. A. Michelsen, G. K. Yue, J. C. Wilson, C. A. Brock, H. H. Jonsson, J. E. Dye, D. Baumgardner, M. H. Proffitt, M. Loewenstein, J. R. Podolske, J. W. Elkins, G. S. Dutton, E. J. Hints, A. E. Dessler, E. M. Weinstock, K. K. Kelly, K. A. Boering, B. C. Daube, K. R. Chan, and S. W. Bowen, The distribution of hydrogen, nitrogen, and chlorine radicals in the lower stratosphere: implications for changes in O<sub>3</sub> due to emission of NO<sub>y</sub> from supersonic aircraft, *Geophys. Res. Lett.*, 21, 2547–2550, 1994.
- Sander, S. P., Friedl, R. R., Golden, D. M., Kurylo, M. J., Huie, R. E., Orkin, V. L., Moortgat, G. K., Ravishankara, A. R., Kolb, C. E., Molina, M. J., and Finlayson-Pitts, B. J.: Chemical Kinetics and Photochemical Data for Use in Atmospheric Studies, 00-3, Jet Propulsion Laboratory, Pasadena, 2000.
- Sander, S. P., Friedl, R. R., Golden, D. M., Kurylo, M. J., Huie, R. E., Orkin, V. L., Moortgat, G. K., Ravishankara, A. R., Kolb, C. E., Molina, M. J., and Finlayson-Pitts, B. J.: Chemical Kinetics and Photochemical Data for Use in Atmospheric Studies, 02–25, Jet Propulsion Laboratory, Pasadena, 2003.
- Sander, S. P., Friedl, R. R., and Yung, Y. L.: Rate of Formation of the ClO Dimer in the Polar Stratosphere – Implications For Ozone Loss. *Science*, 245(4922), 1095–1098, 1989.
- Shindell, D. T. and de Zafra, R. L.: The Chlorine Budget of the Lower Polar Stratosphere - Upper Limits On ClO, and Implications of New Cl<sub>2</sub>O<sub>2</sub> Photolysis Cross-Sections, *Geophys. Res. Lett.*, 22(23), 3215–3218, 1995.

7927

- Shindell, D. T. and de Zafra, R. L.: Chlorine monoxide in the Antarctic spring vortex 2. A comparison of measured and modeled diurnal cycling over McMurdo Station, 1993, *J. Geophys. Res.*, 101(D1), 1475–1487, 1996.
- Solomon, P., Barrett, J., Connor, B., Zoonematkermani, S., Parrish, A., Lee, A., Pyle, J., and Chipperfield, M.: Seasonal observations of chlorine monoxide in the stratosphere over Antarctica during the 1996-1998 ozone holes and comparison with the SLIMCAT three-dimensional model, *J. Geophys. Res.*, 105(D23), 28 979–29 001, 2000.
- Solomon, P., Connor, B., Barrett, J., Mooney, T., Lee, A., and Parrish, A.: Measurements of stratospheric ClO over Antarctica in 1996–2000 and implications for ClO dimer chemistry, *Geophys. Res. Lett.*, 29(15), 1708, doi:10.1029/2002GL015232, 2002.
- Solomon, S.: Stratospheric ozone depletion: A review of concepts and history, *Rev. Geophys.*, 37(3), 275–316, 1999.
- Stimpfle, R. M., Wilmouth, D. M., Salawitch, R. J., and Anderson, J. G.: First measurements of ClOOCl in the stratosphere: The coupling of ClOOCl and ClO in the Arctic polar vortex, *J. Geophys. Res.*, 109(D3), D03301, doi:10.1029/2003JD003811, 2004.
- Troe, J.: Theory of Thermal Unimolecular Reactions At Low-Pressures. 1. Solutions of the Master Equation, *J. Chem. Phys.*, 66(11), 4745–4757, 1977a.
- Troe, J.: Theory of Thermal Unimolecular Reactions At Low-Pressures. 2. Strong Collision Rate Constants – Applications, *J. Chem. Phys.*, 66(11), 4758–4775, 1977b.
- Troe, J.: Predictive Possibilities of Unimolecular Rate Theory. *J. Phys. Chem.*, 83(1), 114–126, 1979.
- Trolier, M., Mauldin, R. L., and Ravishankara, A. R.: Rate Coefficient For the Termolecular Channel of the Self-Reaction of ClO, *J. Phys. Chem.*, 94(12), 4896–4907, 1990.
- von Clarmann, T., Wetzel, G., Oelhaf, H., Friedl Vallon, F., Linden, A., Maucher, G., Seefeldner, M., Trieschmann, O., and Lefevre, F.: ClONO<sub>2</sub> vertical profile and estimated mixing ratios of ClO and HOCl in winter arctic stratosphere from Michelson interferometer for passive atmospheric sounding limb emission spectra, *J. Geophys. Res.*, 102(D13), 16 157–16 168, 1997.
- von Hobe, M., Groö, J.-U., Müller, R., Hrechanyy, S., Winkler, U., and Stroh, F.: A re-evaluation of the ClO/Cl<sub>2</sub>O<sub>2</sub> equilibrium constant based on stratospheric in-situ observations, *Atmos. Chem. Phys.*, 5, 693–702, 2005.
- von Hobe, M., Ulanovski, A., Volk, C. M., Groö, J.-U., Tilmes, S., Konopka, P., Günther, G.,

7928

- Werner, A., Spelten, N., Shur, G., Yushkov, V., Ravegnani, F., Schiller, C., Müller, R., and Stroh, F.: Severe Ozone Depletion in the Arctic Winter 2004/5, *Geophys. Res. Lett.*, in press, 2006.
- Zhu, R. S. and Lin, M. C.: Ab initio studies of  $\text{ClO}_x$  reactions. IV. Kinetics and mechanism for the self-reaction of ClO radicals, *J. Chem. Phys.*, 118(9), 4094–4106, 2003.

7929

**Table 1.** Vibrational frequencies and uncertainties of  $\text{ClOOCI}$ .

Vibrational mode	$\nu$ , $\text{cm}^{-1}$
Torsion	$127^{+0}_{-13}$ <sup>a</sup>
ClOO symmetric bend	$321^{+21}_{-11}$ <sup>b</sup>
ClOO antisymmetric bend	$418.5^c$
Cl—O symmetric stretch	$543.0^c$
Cl—O antisymmetric stretch	$647.7^c$
O—O stretch	$754.0^c$

<sup>a</sup> $127 \pm 20 \text{ cm}^{-1}$  represents the only measurement of the torsional wave number (Birk et al., 1989). As all reported values from ab initio (e.g. Lee et al., 1992) and force field calculations (Jacobs et al., 1994) fall below  $127 \text{ cm}^{-1}$ , we deem it unlikely that the frequency should be higher. The lower limit used here represents the lowest value found in the literature (Jacobs et al., 1994).

<sup>b</sup> $321 \text{ cm}^{-1}$  and upper limit of  $342 \text{ cm}^{-1}$  from different ab initio calculations (Lee et al., 1992), lower limit of  $310 \text{ cm}^{-1}$  from force field calculations (Jacobs et al., 1994).

<sup>c</sup>measured by (Jacobs et al., 1994), in good agreement with other experiments (Burkholder et al., 1990; Cheng and Lee, 1989). Measurements are rather exact and uncertainties of these higher frequencies are not significant for the calculations in the temperature range relevant to this study.

7930

**Table 2.** Standard reaction enthalpies  $\Delta_r H^\circ$  for Reaction (R1) and corresponding heat of formation  $\Delta_f H^\circ$  for  $\text{Cl}_2\text{O}_2$  at 0 K deduced from laboratory and theoretical studies.

	$\Delta_r H^\circ$ (0 K) $\text{kJ mol}^{-1}$	$\Delta_f H^\circ$ (0 K) for $\text{Cl}_2\text{O}_2$ $\text{kJ mol}^{-1}$
Direct determination by photoionisation mass spec.		
Plenge et al. (2005)	$-68.0 \pm 2.8$	$134.1 \pm 2.8$
Deduced from measurements of $K_{\text{eq}}$ as described		
Cox and Hayman (1988)	$-68.9 \pm 0.2$	$133.2 \pm 0.2$
Nickolaisen et al. (1994)	$-70.0 \pm 0.2$	$132.1 \pm 0.2$
Basco and Hunt (1979)	$-68.8$	$132.3 \pm 0.2$
Ellermann et al. (1995)	$-68.6$	$132.5 \pm 0.2$
Ab initio studies		
McGrath et al. (1990)	$-66.1 \pm 17.6$	$136.5 \pm 13.4$
Lee et al., 1992	$-65.2$	$136.9$
Li and Ng (1997)	$-73.9$	$128.2$
Zhu and Lin (2003)	$-78.0 \pm 4.2$	$123.1 \pm 4.2$

7931

**Table 3.**  $K_{\text{eq}}$  values given in the literature. Given are pre-exponential factors and temperature dependence using the JPL format  $K = A \times \exp(B/T)$ .

	$A$	$B$
JPL 2002 <sup>a</sup>	$1.27 \times 10^{-27}$	8744
Cox and Hayman (1988)	$(4.10 \pm 0.31) \times 10^{-30} \times T$	$8720 \pm 360$
Nickolaisen et al. (1994) (3rd law anal.)	$(1.24 \pm 0.18) \times 10^{-27}$	$8820 \pm 440$
Avallone and Toohey (2001)	$1.99 \times 10^{-30} \times T$	8854
von Hobe et al. (2005)	$3.61 \times 10^{-27}$	8167
Plenge et al. (2005)	$1.92 \times 10^{-27}$	$8430 \pm 326$

<sup>a</sup> Factor of 1.3 uncertainty at 298 K and factor of 3 uncertainty at 200 K.

7932

**Table 4.** Overview of parameters used or calculated in Eq. (4) for M=N<sub>2</sub>. Except for  $\beta_c$ , errors given arise mainly from uncertainties in Cl<sub>2</sub>O<sub>2</sub> vibrational frequencies (Table 1).

<i>T</i> K	<i>Z</i> <sup>a</sup> <sub>LJ</sub> 10 <sup>-10</sup> cm <sup>3</sup> molecule <sup>-1</sup> s <sup>-1</sup>	$\rho_{\text{vib,h}}(E_0)^b$ kJ <sup>-1</sup> mol	<i>Q</i> <sub>vib</sub>	<i>E</i> <sub>0</sub> <sup>b</sup> kJ mol <sup>-1</sup>	<i>F</i> <sub>anh</sub>	<i>F</i> <sub>E</sub> <sup>c</sup>	<i>F</i> <sub>rot</sub> <sup>c</sup>	$\beta_c^c$ <sup>d</sup>
200	3.30	2689 <sup>+387</sup> <sub>-147</sub> (2831 <sup>+408</sup> <sub>-154</sub> )	2.02 <sup>+0.16</sup> <sub>-0.03</sub>	68.0 (68.9)	1.52	1.11	12.1	0.55±0.15
250	3.45		2.73 <sup>+0.25</sup> <sub>-0.05</sub>			1.14	9.4	0.49±0.15
300	3.59		3.75 <sup>+0.37</sup> <sub>-0.10</sub>			1.17	7.6	0.45±0.15

<sup>a</sup>Lennard-Jones parameters for Cl<sub>2</sub>O<sub>2</sub> from Bloss et al. (2001) were used.

<sup>b</sup> $\Delta_r H^\circ$  (0 K) from Plenge et al. (2005) is used for *E*<sub>0</sub> (with values based on the Cox and Hayman data, 1988, given in parentheses).

<sup>c</sup>*F*<sub>E</sub>, *F*<sub>rot</sub> and  $\beta_c$  are only marginally affected by the choice of *E*<sub>0</sub>.

<sup>d</sup> we use values of 0.3, 0.45 and 0.6 for  $\beta_c$  (300 K) and derive the temperature dependence as described in (Troe, 1979) with  $\beta_c/(1-\beta_c) \cong -\langle \Delta E \rangle / F_E kT$ , where  $\langle \Delta E \rangle$  is the energy transferred in all up and down transitions.

7933

**Table 5.** Basis of MPIC cross sections at different wavelength intervals.

190–198 nm	data of (DeMore and E. Tschuikow-Roux, 1990)
200–210 nm	mean of the data of (DeMore and E. Tschuikow-Roux, 1990) (Huder and DeMore, 1995)
212–218 nm	mean of the data of (Burkholder et al., 1990) (DeMore and E. Tschuikow-Roux, 1990) (Huder and DeMore, 1995)
220–300 nm	mean of the data of (Cox and Hayman, 1988) (Burkholder et al., 1990) (DeMore and E. Tschuikow-Roux, 1990) (Huder and DeMore, 1995)
302–360 nm	mean of the data of (Burkholder et al., 1990) (DeMore and E. Tschuikow-Roux, 1990)
362–450 nm	log-linear extrapolation of the data at 302–360 nm: log $\sigma$ = -12.982 - 0.01732 $\lambda$

7934

**Table 6.** MPIC cross section data.

$\lambda$ , nm	$\sigma$ , $10^{-20}$ cm <sup>2</sup>	$\lambda$ , nm	$\sigma$ , $10^{-20}$ cm <sup>2</sup>	$\lambda$ , nm	$\sigma$ , $10^{-20}$ cm <sup>2</sup>	$\lambda$ , nm	$\sigma$ , $10^{-20}$ cm <sup>2</sup>
190	565	256	498	322	24.5	388	1.99
192	526	258	451	324	23.0	390	1.83
194	489	260	411	326	21.5	392	1.69
196	450	262	372	328	20.0	394	1.56
198	413	264	341	330	18.0	396	1.44
200	377	266	307	332	16.5	398	1.33
202	344	268	282	334	16.0	400	1.23
204	313	270	259	336	14.5	402	1.14
206	284	272	240	338	14.0	404	1.05
208	257	274	224	340	14.0	406	0.968
210	234	276	204	342	13.0	408	0.894
212	215	278	190	344	12.0	410	0.826
214	205	280	177	346	11.0	412	0.762
216	197	282	163	348	10.2	414	0.704
218	196	284	152	350	9.35	416	0.650
220	195	286	139	352	8.90	418	0.600
222	211	288	128	354	8.30	420	0.554
224	233	290	116	356	7.60	422	0.512
226	267	292	107	358	7.00	424	0.472
228	307	294	97.4	360	6.40	426	0.436
230	351	296	90.9	362	5.60	428	0.403
232	403	298	81.5	364	5.17	430	0.372
234	459	300	73.6	366	4.77	432	0.343
236	511	302	74.0	368	4.41	434	0.317
238	561	304	66.5	370	4.07	436	0.293
240	604	306	59.5	372	3.76	438	0.270
242	634	308	53.5	374	3.47	440	0.250
244	649	310	47.0	376	3.20	442	0.230
246	649	312	41.5	378	2.96	444	0.213
248	639	314	37.0	380	2.73	446	0.196
250	614	316	32.5	382	2.52	448	0.181
252	580	318	29.5	384	2.33	450	0.167
254	541	320	27.0	386	2.15		

7935

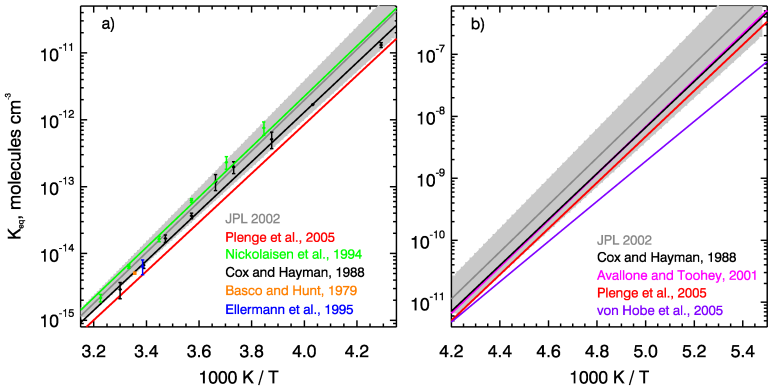


**Fig. 1.** Temperature dependence of  $K_{eq}$  **(a)** in the temperature range of laboratory measurements and **(b)** at stratospheric temperatures. Note that the lines corresponding to the Cox and Hayman (1988) and Nickolaissen et al. (1994) data are based on the fits obtained in this study and not on the fits reported in the original papers. The uncertainty range given by JPL 2002 is shown by the gray areas.

7936



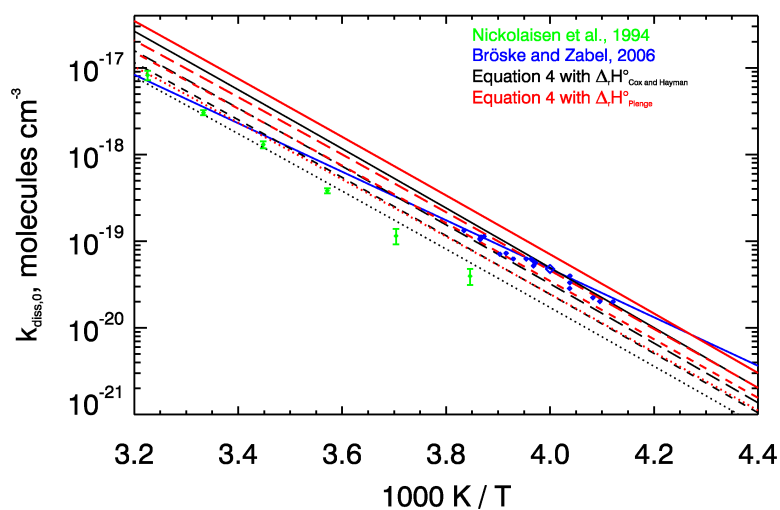


**Fig. 2.** Temperature dependence of  $k_{\text{diss},0}$ . For the theoretical values (Eq. 4), solid lines show  $k_{\text{diss},0}^{\text{sc}}$ , long dashed, short dashed and dotted lines  $k_{\text{diss},0}^{\text{wc}}$  with  $\beta_c$  (300 K) of 0.60, 0.45 and 0.30 respectively.

7937

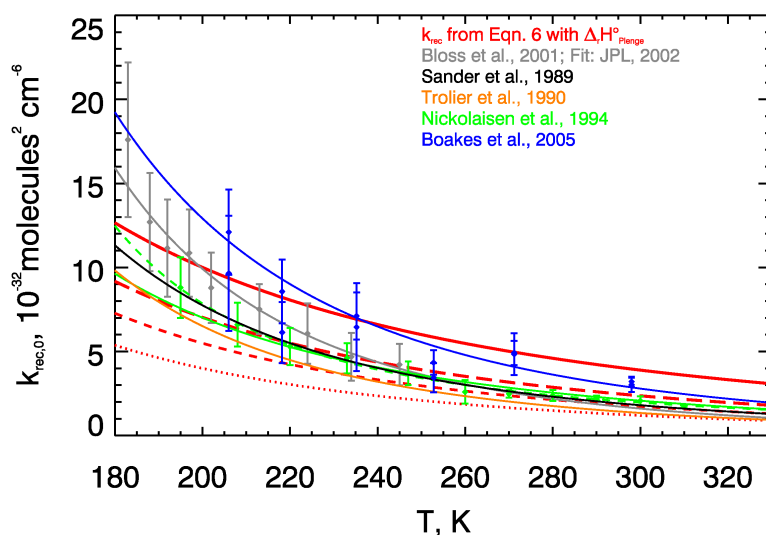


**Fig. 3.** Temperature dependence of  $k_{\text{rec},0}$ . For the theoretical values (Eq. 6), collision efficiencies  $\beta_c$  are represented by line styles as in Fig. 2. For Nickolaissen et al. (1994), the solid line represents the  $T^n$  treatment, the dashed line the  $e^{-E/T}$  treatment. For Boakes et al. (2005) the two points at each temperature represent their results with and without incorporating an intercept in the falloff curves.

7938

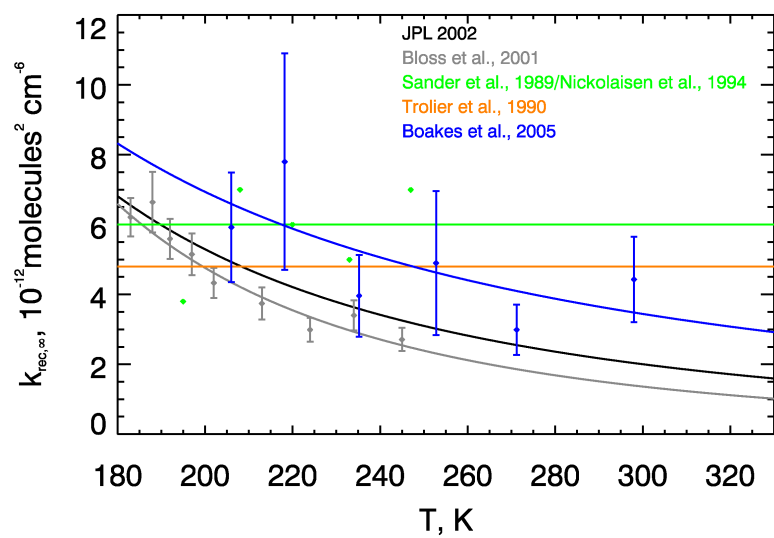


**Fig. 4.** Temperature dependence of  $k_{\text{rec},\infty}$ .

7939

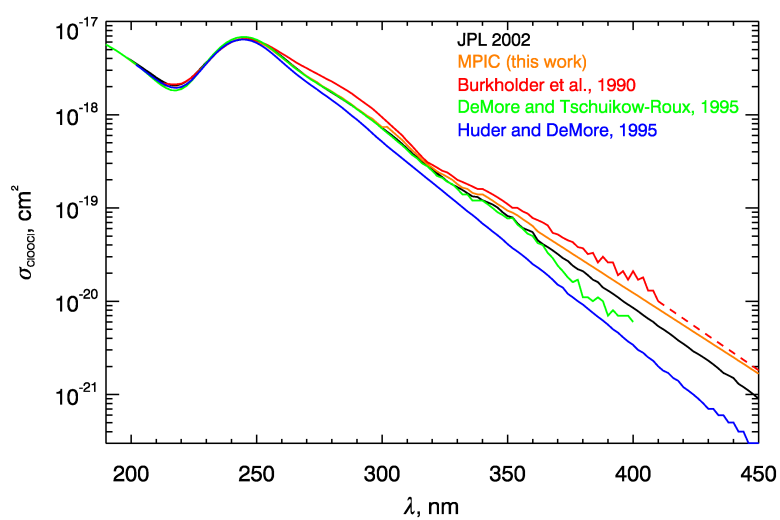


**Fig. 5.** Comparison of UV-Vis absorption spectra of ClOOCl.

7940

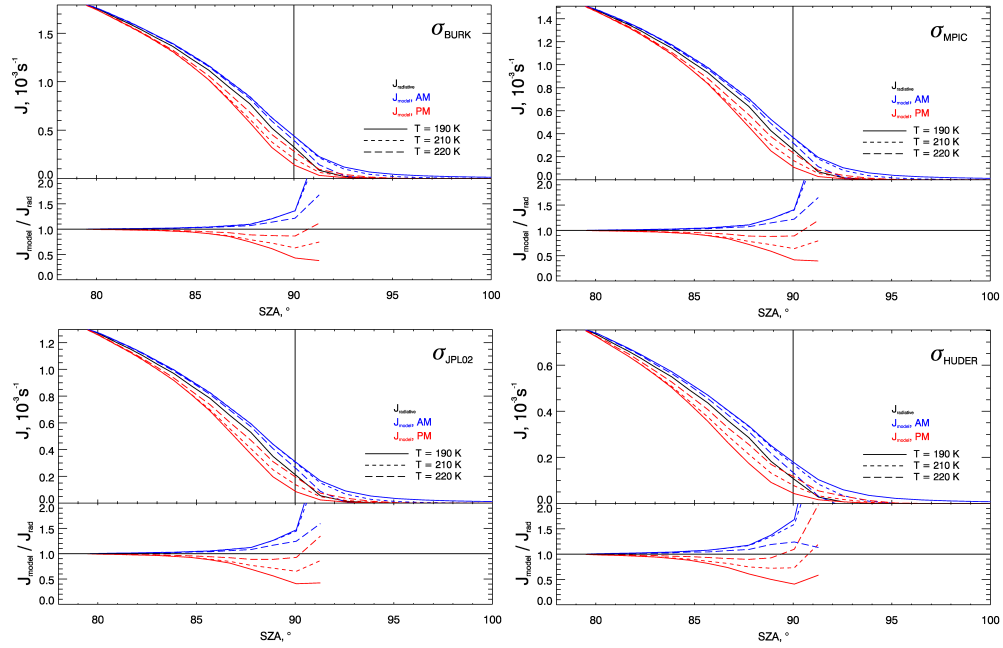


**Fig. 6.** Comparison of  $J$  derived from the simulated abundances of  $[\text{ClO}]$  and  $[\text{Cl}_2\text{O}_2]$  using Eq. (8) to the values from the radiative model for different  $\text{Cl}_2\text{O}_2$  absorption cross sections.

7941

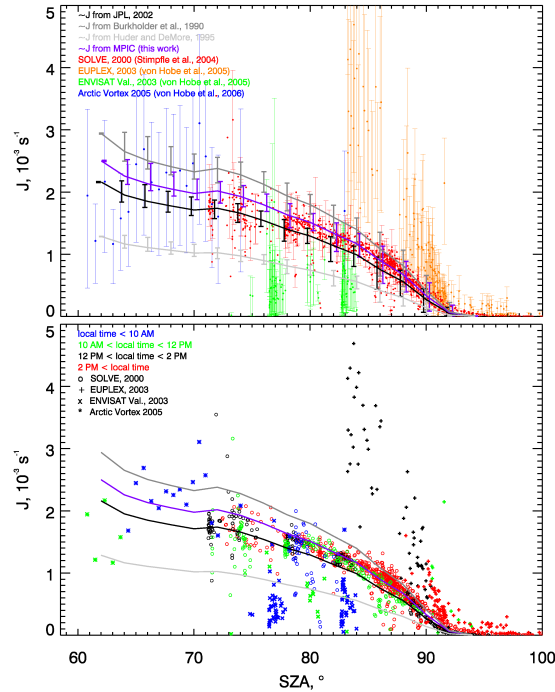


**Fig. 7.**  $J$  values deduced from simultaneous  $[\text{ClO}]$  and  $[\text{Cl}_2\text{O}_2]$  observations (only when  $[\text{ClO}_x] > 200$  ppt and  $P < 120$  hPa) assuming photochemical steady state color coded for the different campaigns with propagated error bars (top panel) and for different times of day (bottom panel). For comparison, average  $J$  values calculated using a radiative model with different  $\sigma_{\text{ClOOC}_1}$  are given for  $2^\circ$  SZA bins, with error indicating maximum and minimum  $J$  in each  $2^\circ$  bin.

7942

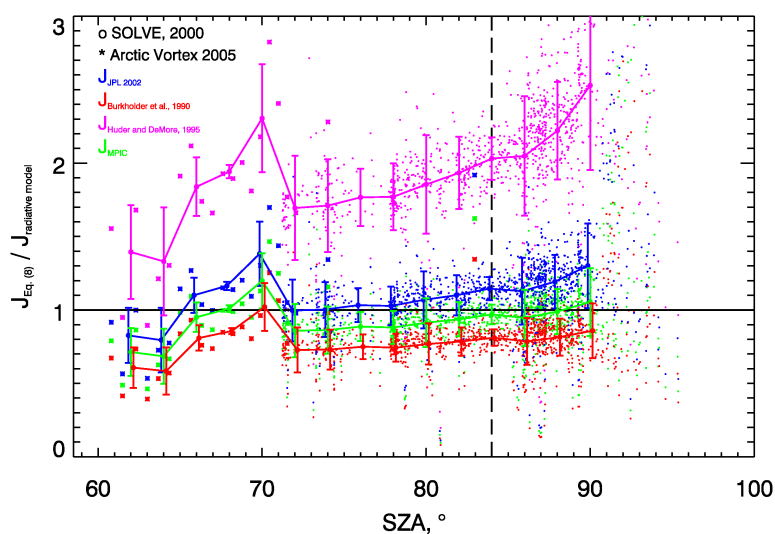


**Fig. 8.** Ratio of  $J$  calculated from SOLVE and VORTEX 2005 observations using Eq. (8) to  $J$  from the radiative model using different  $\sigma_{\text{CIOOCl}}$  vs. SZA.

7943

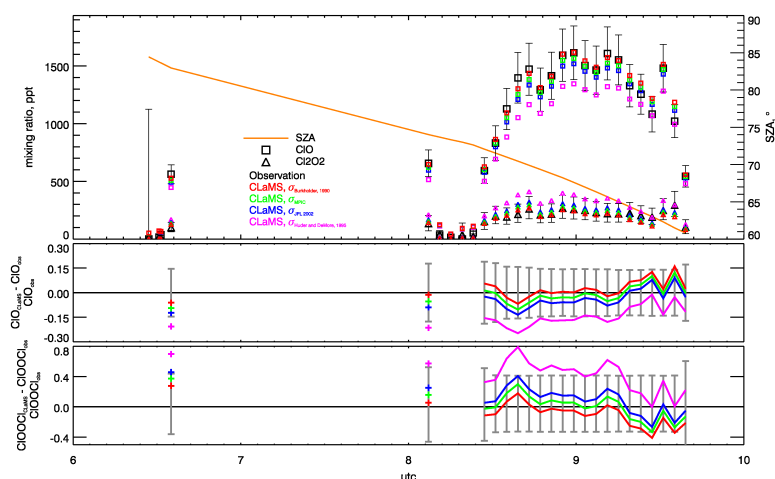


**Fig. 9.** Comparison of simulated CIO and  $\text{Cl}_2\text{O}_2$  using different parameterizations with observations from the Arctic Vortex 2005 flight (von Hobe et al., 2006). For each  $\sigma_{\text{CIOOCl}}$  used in the simulation, the relative difference of the simulated CIO and  $\text{Cl}_2\text{O}_2$  mixing ratios to the observed values is shown in the bottom two panels (except where  $[\text{ClO}_x] < 200$  ppt).

7944